Exergy analysis of a negative CO_2 emission gas power plant based on water oxy-combustion of syngas from sewage sludge gasification and CCS

Ivar S. Ertesvåg [a],*, Paweł Madejski [b], Paweł Ziółkowski [c], Dariusz Mikielewicz [c]

[a] Department of Energy and Process Engineering, NTNU Norwegian University of Science and Technology, Kolbjørn Hejes vei 1b, NO-7491 Trondheim, Norway
[b] AGH University of Science and Technology, Faculty of Mechanical Engineering and Robotics, Department of Power Systems and Environmental Protection Facilities, al. Mickiewicza 30, PL-30-059 Kraków, Poland
[c] Gdańsk University of Technology, Faculty of Mechanical Engineering and Ship Technology, Institute of Energy, ul. G.Narutowicza 11/12, PL-80-233 Gdańsk, Poland

ARTICLE INFO

ABSTRACT

A power cycle with water-injected oxy-combustion (water cycle) is investigated by exergy analysis. It is fueled with syngas (aka. producer gas) from gasification of sewage sludge. The cycle is equipped with a spray-ejector condenser (SEC). CO_2 is separated and compressed for transportation and storage. The net delivered electric power is 31% of the fuel exergy. The task efficiency is 39% when the flue gas bleed to gasification and O_2 penalty are subtracted from fuel, and CO_2 capture is included in the useful product. The large part of exergy destruction, 80%, pertains to the combustor. Increasing the temperature or the pressure of the combustor outlet (turbine inlet) lead, as expected, to reduced exergy destruction and more power delivery. Reducing pressure of the gas turbine outlet (SEC inlet) also increases power production. Varying pressure and temperature of the SEC outlet affects the distribution of exergy destruction among units of the condenser, however scarcely the overall efficiency. Reducing the ambient temperature, including cooling water temperature, reduces the efficiency of the plant, contrary to the effect of conventional plants. The reason is that the low pressure of SEC relies on the pressure and mass flow of injected water, rather than the temperature.

1. Introduction

The background of this work is twofold: First, handling of sewage sludge poses a considerable environmental challenge to urban societies. Second, CO_2 emissions contribute to global warming. Sewage sludge is biomass and can be converted to combustible gases to fuel a thermal power plant. If oxy-combustion (aka. oxy-fuel) technology is used, the produced CO_2 can be sequestered and stored to avoid CO_2 emissions. As biomass (here sewage) is regarded carbon neutral, the sequestering makes the plant CO_2 negative.

The present paper is part of a project nCO2PP [1], aiming at realizing a negative CO_2 power plant. The process has been presented previously [2], with mass and energy analysis. Here, an exergy analysis (1st and 2nd law analysis) will be conducted and presented. The developed cycle consists of innovative units such as a wet combustion chamber (WCC) and a spray ejector condenser (SEC) with water/CO_2 separator, designed and developed under the project nCO2PP [1].

The energy analysis previously performed [2] allows to evaluate the overall process efficiency, taking into account the internal efficiency of individual cycle units. The exergy analysis results give new insight into the comprehensive process analysis by identifying and quantifying the thermodynamic losses and deficiencies of the process. Thereby, dedicated actions to improve the process can be made.

For mature technical systems, like the conventional gas-turbine cycle, the effective actions for improvement are usually well known by the relevant industry. However, for new solutions, like those presented here, the improvement potentials are not known and may not be obvious in the first place. For such systems, exergy analysis provides useful insight into the thermodynamic losses and, hence, the possibilities for improvement.

An example can be found in [3], where optimum operating parameters were determined based on exergy analyses with emphasis on the economics and emissions of the unit. Another example is combined cycle units with steam injection [4], where a two-pressure heat recovery steam generator was analyzed, showing that there is a definite relationship between the amount of steam injected into the combustion chamber and the air flowing in the nominal state, when the highest energy and exergy efficiencies are achieved. Another solution is to

* Corresponding author.
E-mail addresses: Ivar.S.Ertesvag@ntnu.no (I.S. Ertesvåg), Pawel.Madejski@agh.edu.pl (P. Madejski), Pawel.Ziolkowski1@pg.edu.pl (P. Ziółkowski), Dariusz.Mikielewicz@pg.edu.pl (D. Mikielewicz).

make the combined-cycle gas-turbine (CCGT) cogeneration unit more flexible for different types of retrofits. This was chosen for the unit in Gorzów Wielkopolski, where two types of steam injection into the combustion chamber were analyzed [5]. It was shown that higher exergy losses in the combustion chamber occur for the steam-injection solution, but also that it is more flexible. Of course, there are optimizations in the literature for gas turbines alone [6,7], but a much broader range of analyses needs to be carried out for CCGT units that aim to capture carbon dioxide. Here, we traditionally distinguish between three technologies, namely post-combustion [8,9], pre-combustion [10] and oxy-combustion [11,12]. Detailed exergetic analyses for several cases of CO_2 capture by chemical absorption and CO_2 compression systems were presented in [8], and a configuration was obtained in which the exergetic losses were at the lowest level with simultaneous preparation of CO_2 for sequestration. Also systems with pre-combustion capture should be analyzed exergetically as surprising results can be obtained: for example, that a single heat exchanger with unfavourable temperatures was the second most exergy-destructive unit of the system (after the combustor) [10]. Such information provides a reliable basis for optimizing the process and avoiding exergy losses to the environment. A system [11] with similarities to the one considered in the present paper concerns oxy-combustion, where the predominant role in the working medium is played by CO_2. In oxy-combustion, oxygen separation from air is an important sub-process, which was analyzed and optimized by exergy analysis by [13].

The presented cycle is based on combustion in an oxygen atmosphere, giving mainly CO_2 and water vapour. The CO_2 capture method is to use a direct-contact heat exchanger to condense steam and, thereby, separate CO_2. Essentially, it is a water cycle. Variants of this cycle were analyzed by [14,15] on energy basis, and with exergy by [16,17]. The present system is, however, simpler and more compact than those previously investigated.

At this point, it is worth noting that in general, system zero-emissions can be achieved in two ways in combustion plants, namely: (1) burn fossil fuel and capture CO_2; and (2) burn fuel from renewable sources, such as sewage sludge gasification. However, the combination of both techniques, capture CO_2 from a renewable source, will lead to a system with a negative carbon footprint.

The aim of this study was to conduct a comprehensive exergy analysis of the plant suggested in the nCO2pp project [1], with variation of key parameters and discussion with respect to 2nd-law considerations. The purpose of the exergy evaluation was to localize and quantify the thermodynamic deficiencies of the processes and hence, contribute to the overall improvement of the plant. Moreover, the 2nd-law (exergy) analysis also implies a realizability assessment. Besides the level of detail, the deviations, hence novelty, from previous water-cycle analyses are that the present cycle interacts with a gasification reactor for the syngas fuel, that it has no 2nd combustor for reheat between gas turbines, and that it has a spray ejector condenser. The latter is supposed to be considerably more compact than a conventional recuperating condenser.

In the following two sections, the process and its modelling are described. The chosen operational conditions and parameter variations are described in Section 4. Results will be presented and discussed in Section 5, before conclusions are made in the final section.

2. Process description

The negative CO_2 emission power plant is based on gasification of sewage sludge and combustion of the producer gas (aka. syngas) with pure oxygen (not air). To reduce the temperature of the combustion and of the resulting flue gases, liquid water is injected into the combustion chamber. Thus, it is a wet combustion chamber (WCC) in a water-cooled oxy-fuel combustion process. The cost of O_2 production required a fuel-oxygen ratio close to stoichiometric.

The power plant process is shown in Fig. 1. The flows of fuel (Stream 0^{Fuel}) and oxygen (Stream 0^{O2}) are compressed in compressors C-oxy and C-Fuel from the inlet pressures to combustor injection pressure and fed (Streams 1^{Fuel} and 1^{O2}) to the WCC. The flue gas (Stream 2) is expanded through gas turbines GT1 and GT2 and then used to heat (HE1) water for the WCC. The gas turbines power the fuel and oxygen compressors, a pump (P-H2O) and an electric generator (G). Assuming complete combustion with stoichiometric oxygen, the flue gas (Streams 2 to 5) consists of H_2O and CO_2.

The low-pressure gas flow (Stream 5) is ducted to the spray ejector condenser ("EC" in the flowsheet), where it is brought to a higher pressure by interaction with the injected motive fluid (Stream 1^{SEC}) delivered by the water pump (P-EC). Vapour is condensed by direct contact with the subcooled injected water. The further step is cooling of the water/CO_2-mixture (Stream 2^{1-SEC}) by low-temperature cooling water (Streams 0^{LTS} to 2^{LTS}, with pump P-LTS) in heat exchanger HE2. In the cooled stream (2^{2-SEC}), most of the H_2O is condensed. This liquid is separated (Stream 6) in a separator (S) and directed out of the system (Stream 1^{Prod}) or re-used for injection to the SEC or the WCC. The remaining CO_2-rich gas (Stream 1^{CCU}) is compressed (compressors C1-CO2 and C2-CO2) and cooled (HE3, HE4) before it is removed beyond the system boundary (Stream 5^{CCU}) as a liquid. A minor amount of remaining water condenses and is removed after the 2nd stage of compressing/cooling (Stream 0^{Prod}). It is included in the water discharge, Stream 2^{Prod}. Electric motors (M) run the pump (P-EC) and the CO_2 compressors. The separated and re-used water is pumped partly through heat exchangers HE4 and HE3 (Stream 3^{H2O}) to be heated by the compressed CO_2-rich gas, and partly through HE1 (Stream 1^{H2O}) to be heated by the flue gas, before injection to the WCC.

The syngas fuel (aka. producer gas) is produced from sewage sludge in the gasifier. Some flue gas (Stream 0^R) is bled between the first and second gas turbines to be used as a gasifying agent in the gasifier.

3. Thermodynamic modeling of the negative-CO_2 emission cycle

3.1. Simulation model of the process

The cycle described in the previous section was simulated using the software Ebsilon Professional [18]. The code solved the species, mass and energy balances for each subsystem (unit) and for the overall system.

The exergy calculations of Ebsilon did not consider changes in composition, as chemical exergy was not evaluated. Accordingly, such calculations had to be supplemented by the investigators, see next section.

The systems were assumed as steady-state steady-flow processes. Fuel and pure oxygen were assumed continuously available at the given inflow states. Each unit was assumed adiabatic. The combustion was assumed complete, converting all carbon to CO_2 and all hydrogen to H_2O.

In the spray-ejector condenser, the flow rate of the motive fluid (Stream 1^{SEC}) was chosen based on the procedure described in [2]. In the separator model, an assumption of full gas/liquid separation was made. Models of other cycle units (compressor, pump, and heat exchanger) were adopted to calculate the design size based on the input data of mass flow rate, temperature and pressure.

3.2. Evaluation of exergy in flows of the power cycle using Ebsilon professional

Flow exergy is the work theoretically obtainable when the flow is brought to total equilibrium with the environment. That is, in form of gases found in the stable atmosphere (N_2, O_2, H_2O, CO_2 and noble gases) at their respective partial pressures, $p_i^e = X_i^e p_0$, and the temperature, T_0, in the ambient atmosphere. Here, X_i^e is the mole fraction of a gas in the atmosphere. The ambient conditions, or atmosphere, can
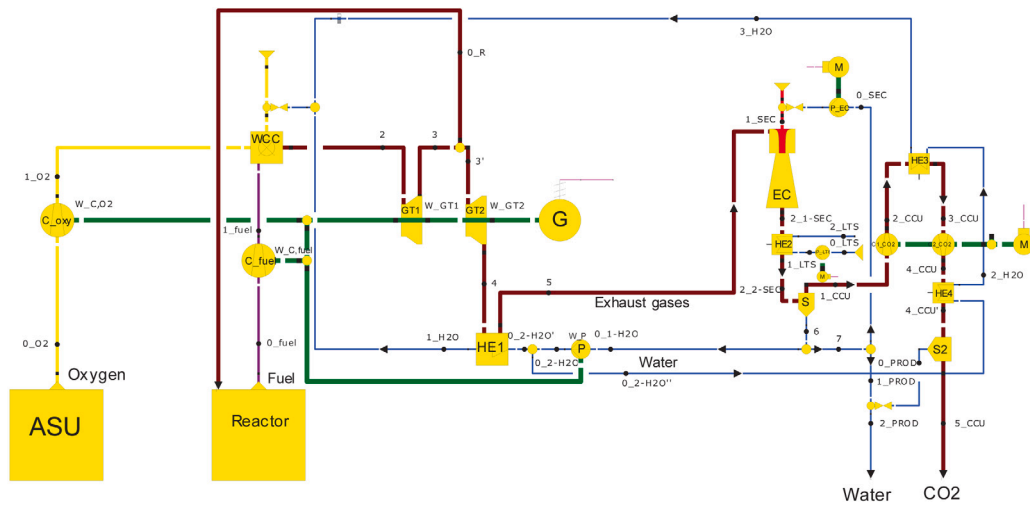
Fig. 1. Process flow diagram of the negative-CO_2 emission gas cycle, generated by process simulation software Ebsilon Professional [18].

be defined by specifying temperature (T_0), pressure (p_0) and relative humidity (ϕ^e) [19,20]. The flow exergy is customarily decomposed into a thermomechanical ("tm") part and chemical exergy. The latter is composed of a mixing part ("mix") and the component (species) chemical exergies:

$$\dot{E} = \dot{E}^{tm} + E^{ch} = E^{tm} + E^{ch,mix} + E^{ch,s}. \tag{1}$$

This can be elaborated as

$$\dot{E} = \underbrace{(\dot{H} - \dot{H}_0) - T_0(\dot{S} - \dot{S}_0)}_{(I)}$$
$$+ \underbrace{\left(\dot{H}_0 - \sum_i \dot{n}_i \bar{h}_{i,0} \right) - T_0 \left(\dot{S}_0 - \sum_i \dot{n}_i \bar{s}_{i,0} \right)}_{(II)} + \underbrace{\sum_i \dot{n}_i \bar{e}_i^{ch}}_{(III)}. \tag{2}$$

Here, $\dot{H} = \dot{H}(T, p, \dot{n}_i)$ and $\dot{S} = \dot{S}(T, p, \dot{n}_i)$ are the rates of enthalpy and entropy for the mixture, subscript 0 denotes that they are evaluated at the restricted dead state (T_0, p_0, for the mixture), while $\bar{h}_{i,0} = \bar{h}_i(T_0, p_0)$ and $\bar{s}_{i,0} = \bar{s}_i(T_0, p_0)$ are, respectively, the enthalpy and entropy per mole of the pure species at the restricted dead state. Differences in kinetic and potential energy are neglected. $\dot{n}_i$ and $\bar{e}_i^{ch}$ are, respectively, the molar flow rate and the molar chemical exergy of species i.

The present study was based on the energy analysis conducted with the Ebsilon code [18], which included an exergy calculator. It evaluated the reversible work when the flow is brought from the actual state to the restricted dead state, that is, (T_0, p_0). Hence, Ebsilon exergy equals Term (I) of Eq. (2). The remaining terms have to be evaluated separately, when relevant.

Due to condensing and phase separation when the stream includes H_2O, the mixture is partly separated. This means that the Ebsilon exergy calculation can be interpreted as including a part of the mixing exergy, together with the thermomechanical part. Thus, the total flow exergy rate can be evaluated as the quantity obtained from the simulator Ebsilon, here denoted, $\dot{E}^{sim}$ and the remaining part, which has to be calculated separately:

$$\dot{E} = \dot{E}^{sim} + (\dot{E} - \dot{E}^{sim}) \tag{3}$$

For a general flow containing H_2O with mole fraction $X_{H_2O} > p_{s0}/p_0$ (no other substances condensing at the restricted dead state), the remaining part can be expressed as

$$\dot{E} - \dot{E}^{sim} = T_0 \bar{R} \left(\sum_{i \neq H_2O} \dot{n}_i \ln X_{i0} + \dot{n}_{H_2O} \ln \frac{p_{s0}}{p_0} \right)$$
$$+ \dot{n}_{H_2O(liq,0)}(p_0 - p_{s0})\bar{v}_{f0} + \sum_i \dot{n}_i \bar{e}_{i(g)}^{ch} \tag{4}$$

Here, $\bar{R}$ is the universal gas constant, $\dot{n}_i$ is for the actual mixture. $\dot{n}_{H_2O(g0)}$ and $\dot{n}_{H_2O(liq0)}$ are, respectively, the molar flow rates of gaseous and liquid H_2O in the mixture when it is brought to the restricted dead state (T_0, p_0), while X_{i0} is the mole fraction for species i of the gaseous phase at this state. These quantities are determined by setting the partial pressure of vapour H_2O equal to the saturation pressure at T_0 and by assuming that no gas is dissolved in the liquid. p_{s0} and $\bar{v}_{f0}$ are, respectively, the saturation pressure and saturated-liquid molar volume for H_2O at T_0. In the final term, it is emphasized that for H_2O, the component molar chemical exergy for gaseous state (g) is the relevant quantity in this expression, regardless of the phase of H_2O in the actual or restricted dead states.

For a flow without condensation at the restricted dead state ($X_{H_2O} \leq p_{s0}/p_0$), the expression simplifies to

$$\dot{E} - \dot{E}^{sim} = T_0 \bar{R} \sum_i \dot{n}_i \ln X_i + \sum_i \dot{n}_i \bar{e}_i^{ch}. \tag{5}$$

Here, the first right-hand side term is the mixing exergy of an ideal mixture. This term is negative, and it represents the exergy penalty of mixing the substances. For the streams with a single pure species, the right-hand side of Eq. (5) reduces to the chemical exergy of that component.

3.3. Energy and exergy analysis of the developed processes

As noted above, the elemental, mass and energy balances were taken care of by the simulator, Ebsilon. The exergy balances had to be supplemented, as well as chemical exergy calculations for each stream. For each unit (assumed steady state and adiabatic), the exergy balance was expressed as

$$0 = \sum_j \dot{E}_{j,in} - \sum_j \dot{E}_{j,out} - \dot{W} - \dot{E}_d. \tag{6}$$

Here, index j denotes a stream identifier, "in" and "out" refers to inflow and outflow of the unit, $\dot{W}$ is the power (work rate) delivered by the unit and $\dot{E}_d$ is the exergy destruction rate. Exergy rate associated with heat transfer to the units was not relevant with the present assumptions. The work rates were obtained in the energy analysis (enthalpy rate differences), while the flow exergy rates were obtained as described above. The exergy destruction then appeared as the remaining quantity to resolve from the exergy balance.

3.4. Oxygen separation, syngas fuel supply, exergy discharge and carbon dioxide capture

In the simulator model, the stream of pure O_2 used for oxy-combustion was regarded as an inflow to the process. The air-separation

Table 1
Chemical exergies at ambient conditions 15 °C, 1 atm (1.01325 bar), 60% relative humidity [19].

Species	$\bar{e}_j^{ch}$ (kJ/kmol)
O_2	3770
CO_2	18924
$H_2O(g)$	11010
$H_2O(liq)$	1224
H_2	238157
CO	275131
CH_4	834227
C_3H_8	2154890

unit (ASU) was not simulated in detail. However, the cost of the separation (and some pressurizing) was included in the analysis by estimating the electric energy (exergy) required for the process and subtracting this from the gross power generation.

Also the fuel stream was regarded an inflow to the simulated process. The gasifier providing syngas fuel required a bleed of flue gas from the process. The remaining exergy required for the gasification process was provided by the sewage sludge and not accounted for in the present analysis.

The mass flow rate of water in the cycle was increased by the reaction product H_2O, which then was the net discharge. With a near-ambient state, its exergy was primarily the chemical exergy. Furthermore, some thermal energy was discharged from heat exchanger HE2 by cooling water taken from the environment. The exergy associated with this discharge implied exergy destruction when mixed into the environment. Although this occurred outside the control volume, it was a result of the process.

The resulting stream of compressed and concentrated CO_2 was delivered at a high pressure. The thermodynamic asset of this stream is the sum of the pressure part of the thermomechanical exergy, i.e.,

$$\dot{E}^{tm,p} = (\dot{H}(T_0, p, \dot{n}_i) - \dot{H}_0) - T_0(\dot{S}(T_0, p, \dot{n}_i) - \dot{S}_0), \tag{7}$$

and the chemical exergy. The further handling of this stream (e.g., piping or shipping for deposit) was not part of this study.

4. Present predictions

4.1. Ambient conditions, fuel and oxygen supplies

Unless otherwise specified, the ambient conditions (local atmosphere) were chosen as temperature $T_0 = 15\,°C$ (288.15 K), pressure $p_0 = 1\,atm$ (1.01325 bar) and relative humidity $\phi^e = 0.60$. These conditions aligned with the ISO standard conditions for gas turbine testing [21]. Also cooling water was assumed available at the ambient temperature and pressure.

The syngas mixture (aka. producer gas) from sewage sludge gasification [22] was assumed with a composition (molar based) of CO: 9.32%, CO_2: 26.44%, CH_4: 13.92%, C_3H_8: 3.50% and H_2: 46.82%. In addition, for comparison, the process was also simulated with natural gas (simplified as pure CH_4) as the fuel. The supplies of syngas and methane were assumed at the ambient pressure and temperature.

The chemical exergies for the specified ambient conditions were evaluated with the model of [19] and presented in Table 1. The syngas fuel mixture had a chemical exergy of 330534 kJ/kmol (mixture exergy included). The lower heating value (LHV) of the syngas was 17090 kJ/kg, and the molar mass was 18.97 kg/kmol, as provided by the simulator.

In the gasifier, steam is used as a gasifying agent or converter [2,22, 23]. For this purpose, a fraction of the flue gas stream was bled between the two gas turbines. The amount was set to 0.83 mol bleed flue gas (with 0.73 mol of H_2O) per mol of consumed syngas [23]. According to results of [23], the precise amount of CO_2 in the bleed had minor

influence on the syngas parameters compared to feedstock, temperature and pressure of the reactor.

The supply of pure O_2 used in oxy-combustion comes with a cost. The chemical exergy of the pure species constitutes the minimum thermodynamic requirement to produce it from the environment, i.e., the atmosphere. The actual requirement is higher. Based on recent studies [24,25], the specific power consumption was set to 25.3 MJ/kmol (0.220 kWh/kg) for O_2 at the combustor inlet pressure. The pressure was achieved by pumping liquid O_2 before evaporating within the air-separation unit. Thus the penalty was approximated to this value for all the investigated combustor pressures. The impurity of 0.2% argon was neglected. The data represented a moderate improvement from those observed by [2] and those found by [13]. Including the thermomechanical exergy, the separation process had an efficiency of 14.3%. The required power, or exergy penalty, of the separation was subtracted from the gross power production of the power plant.

4.2. Numerical simulation of gas power cycle using thermodynamic models

In the thermodynamic model of Ebsilon [18], the Redlich–Kwong–Soave real gas formulation [26] was used. This model has been found [27] to give relatively low errors for H_2O–CO_2 mixtures. For flows of pure water/steam, data of IPAWS-IF97 [28] were used.

The equations of state, mass and energy balances were resolved iteratively, with a convergence criterion set to 10^{-9}. This referred to the relative deviation between the second-last and the last iteration step for mass flow, pressure and enthalpy.

The thermodynamic models of Ebsilon used the convention of setting the enthalpy zero point for gaseous flows like air and flue gas at 0 °C. It can be noted that the enthalpy values displayed by Ebsilon did not balance for reactors and separators, i.e., when composition change. This affected postprocessing based on output quantities, while computations within the simulator appeared to be correct.

Following [2], the isentropic efficiencies were assumed as 0.89 for the turbines, 0.87 for the compressors and 0.43 for the pumps. The mechanical efficiencies for rotating machinery were set to 0.99, while the electric efficiencies of generator and motors were set to 0.9856 and 0.85, respectively.

The pressure losses in heat exchangers were set to 3% at the liquid side and 25 mbar on the gaseous side [29]. The temperatures of heat exchangers HE1, HE3 and HE4 were set for each case. The minimum temperature differences were not less than 20 K, 75 K and 45 K, respectively, except when the SEC inlet temperature was reduced (13 K difference at 32 °C SEC inlet temperature). For HE2, the minimum temperature difference was set to 3 K, with an exception at a reduced SEC outlet temperature.

4.3. Base case

The Base Case was designed to approximately 2 MW of electric power. The choice was motivated by, among other, aiming at a size of the powerplant to fit into a module that can be transported and installed as a unit. It can be noted that the analysis of [2] was based on a prototype size of approximately 100 kW electric power.

The turbine inlet (combustor outlet) temperature was set to 1100 °C and the pressure to 10 bar. The injection pressures of fuel and oxygen to the combustor was set to 1.05 times the combustor pressure. For water injection, the pressure from the water pump (P) was set to 30.9 bar to keep the flow in liquid state through heating (HE1, HE3, HE4).

The outlet of the first gas turbine (GT1) was set to 1.02 bar, due to the bleed of flue gas to the gasifier. The outlet of the second gas turbine was related to the conditions of the spray ejector condenser(SEC), and the pressure was set to 0.078 bar. The temperature of the flue gas inflow to the SEC was set to 40 °C.

The water inlet to the spray ejector condenser was set to 6 bar. Its temperature was dependent on the temperature of the outflow from condenser and separator.

Table 2

Data for selected positions in the flowsheet: molar mass, composition (mole fractions) of the streams. Base Case, syngas and methane.

Stream	Fuel: syngas				Fuel: methane			
	Molar mass (kg/kmol)	CO_2 (mol%)	H_2O (mol%)	$\bar{e}^{ch}$ (kJ/kmol)	Molar mass (kg/kmol)	CO_2 (mol%)	H_2O (mol%)	$\bar{e}^{ch}$ (kJ/kmol)
2	21.082	11.796	88.204	11943	20.143	8.189	91.815	11658
$2^{1\text{-SEC}}$	18.031	0.0621	99.938	11015	18.027	0.0441	99.956	11014
1^{CCU}	43.483	97.974	2.026	18763	43.483	97.974	2.026	18763
5^{CCU}	43.922	99.662	0.338	18897	43.922	99.662	0.338	18897

The pressure of the outflow CO_2-rich stream (Stream 5^{CCU}) was set to 78 bar. This is above critical pressure, which means that a potential further pressure increase can be achieved by pumping. The temperature was set to 90 °C for the syngas case and 63 °C for methane. The difference was due to the reduced mass flow rate for GT2 after bleed to the gasifier.

4.4. Parameter variations

To investigate the described system, and to understand the exergy conversion and destruction, some selected parameters were varied. It is noted that the analyses are at the design level, not operational. That is, the variations represent changed devices (when relevant), not changed conditions for the same device or geometric parameters.

– The turbine inlet (combustor outlet) temperature was varied as 850, 950, 1050, 1100 (BC) and 1150 °C ("BC" denotes the Base Case).
– Combustor (turbine inlet) pressure: 6, 10 (BC), 16, 25 and 40 bar.
– GT2 outlet pressure: 0.068 (BC), 0.078, 0.088 and 0.100 bar (the corresponding inlet pressures to SEC were 0.025 bar lower). This was achieved by changing the GT2 pressure ratio, while the GT2 inlet pressure was maintained constant because of the bleed to the gasifier.
– Flue gas temperature to SEC (Stream 5): from 32 to 120 °C (BC: 40 °C). The pressure was maintained at 0.053 bar. The variation was obtained by reducing the heat transfer in HE1; i.e., lesser mass flow rate and/or temperature rise of water.
– Discharge pressure from SEC (Stream $2^{1\text{-SEC}}$): 1.0, 1.015, 1.030, 1.045 (BC), 1.060, 1.075, 1.090, 1.105 bar.
– Temperature out of HE2 (Stream $2^{2\text{-SEC}}$): 16, 17, 18 (BC), 19, 20 °C. This was also the temperature of the motive water inlet to SEC (Stream 1^{SEC}). The variation was achieved by adjusting the mass flow rate of Stream 1^{SEC}.
– Ambient temperature: 0.01, 5, 10, 15 (BC), 10, 25 and 30 °C. This temperature applied to cooling water, fuel and O_2 supply. The ambient pressure (1 atm) and relative humidity (60%) were not varied.

For comparison, the power plant was simulated with methane as fuel. The chosen parameters were maintained. The comparison was made on the basis of maintained volumetric flow through the first gas turbine. This implied that the methane-fueled version had a slightly higher rate of converted LHV. Methane required no bleed of flue gas.

5. Results and discussion

5.1. Base case

The flow of captured and compressed CO_2 is a desired product of the process. The exergy is the thermodynamic value of the flow. It therefore represents a useful product of the process, along with the net power output. The chemical exergy and pressure part of thermomechanical exergy of the product CO_2 was 3.9% of the chemical exergy of syngas, while 3.2% for methane.

Table 2 shows composition data for selected streams of the Base Case. Other streams can be found from these data. The gas-phase fractions in Streams $2^{1\text{-SEC}}$ and $2^{2\text{-SEC}}$ were 0.1087% and 0.1085%, respectively, on mass base. The other streams were single-phase flows.

Temperature, pressure, mass flow rate and exergy flow rate for all streams of the Base Case are shown in Table 3. The exergy flow rates are expressed as fractions of the fuel chemical exergy rate, which were 6757.8 kW and 7133.8 kW, respectively, for syngas and methane. It should be noted that for the cooling water (Streams 0^{LTS}, 1^{LTS} and 2^{LTS}), the chemical exergy of liquid water was not included. This was because this water is just a medium for heat exchange, with no other participation in the process (cf. discussion on through-flow exergy in [30,31]).

Main data for the power plant are provided in Table 4.

Exergy efficiencies, ψ, were evaluated as task efficiencies [31,32]. That is the exergy rate of the desired product as a fraction of the exergy rate utilized by the unit. For heat exchangers it is the exergy rate change of the cold flow divided by that of the hot flow. For compressors and pumps it is the ratio of increased flow exergy rate to supplied power, and for turbines it is the ratio of power produced by the decreased flow exergy rate. For SEC and WCC, the task exergy efficiency is the outflow exergy divided by the inflow exergy. For the overall plant, the desired products are the delivered electric power and the exergy rate of captured/compressed CO_2, while the utilized exergy is the fuel and O_2 exergy subtracted bleed exergy and O_2 penalty.

Table 5 shows process unit results of the Base Case: utilized exergy rate and exergy destruction rate as fractions of the fuel chemical exergy rate, together with the task exergy efficiency. In particular, it can be noted that for SEC, most of the utilized exergy (here: inflow exergy) was component chemical exergy of the water, Stream $2^{1\text{-SEC}}$, which was flowing through the device; that is, 331% of the fuel chemical exergy for the syngas case.

5.2. Distribution of exergy destruction and output: parameter variation

In the following graphs, the distribution of the exergy is grouped as
– exergy destruction in the combustor ("WCC" in the graphs).
– exergy destruction in heat exchanger HE1 and pump with electric motor ("HE1").
– exergy destruction in fuel compressor, gas turbines and electric generator ("GT").
– exergy destruction in SEC, HE2 and pumps P-SEC and P-LTS with motors ("SEC").
– exergy destruction in CO_2 compressors with motors, HE3 and HE4 ("CprCO2").
– exergy discharged by produced water (Stream 2^{Prod}), cooling water (Stream 2^{LTS}) and the temperature part of thermomechanical exergy of the captured and compressed CO_2 (cf. Eq. (7)) ("Disch").
– exergy in flue gas bleed to gasification reactor, Stream 0^R ("Bleed").
– exergy (electric energy) used for O_2 separation, i.e., O_2 penalty ("O2 pen").
– net electric energy (exergy) delivered from the power plant ("El pow").
– exergy of captured and compressed CO_2, i.e., chemical exergy and the pressure part of thermomechanical exergy ("CO2").

All exergy rates are expressed as a fraction (in %) of the flow rate of chemical exergy of the fuel supplied to the combustor. For compressors, pumps and turbines, mechanical losses were included in the exergy destruction.

It can be noted that the discharge fractions are very small and hardly visible in the graphs.

Table 3

Data for streams in the flowsheet: temperature, pressure, mass flow rate and total exergy flow rate (in % of the fuel chemical exergy). Base Case.

Stream	Fuel: syngas				Fuel: methane			
	T (°C)	p (bar)	$\dot{m}$ (kg/s)	$\dot{E}/\dot{E}_{fu}^{ch}$ (%)	T (°C)	p (bar)	$\dot{m}$ (kg/s)	$\dot{E}/\dot{E}_{fu}^{ch}$ (%)
0^{Fuel}	15	1.01325	0.38778	100.00	15	1.01325	0.137185	100.00
1^{Fuel}	252.0	10.5	0.38778	102.41	224.1	10.5	0.137185	100.93
0^{O2}	15	10.5	0.48026	2.08	15.0	10.5	0.54727	2.24
1^{O2}	15	10.5	0.48026	2.08	15.0	10.5	0.54727	2.24
$0^{1\text{-}H2O}$	18	1.02	1.33091	1.45	18	1.02	1.4400	1.49
1^{H2O}	220.80	30.9	1.03091	4.51	224.4	45.0	1.1900	5.06
3^{H2O}	175.97	29.07	0.300	0.96	175.9	44.1	0.250	0.77
2	1100	10	2.1985	66.66	1100	10	2.12445	63.36
3	676.50	1.02	2.1985	36.28	672.7	1.02	2.12445	34.29
0^{R}	676.50	1.02	0.35676	5.89				
4	324.84	0.078	1.84219	11.15	319.0	0.078	2.12445	12.40
5	40	0.053	1.84219	5.34	40	0.053	2.12445	5.98
0^{SEC}	18	1.02	297.293	323.77	18	1.02	351.223	362.35
1^{SEC}	18.04	6	297.293	325.97	18.04	6	351.223	364.81
$2^{1\text{-}SEC}$	20.92	1.045	299.135	329.02	21.1	1.045	353.347	367.43
$2^{2\text{-}SEC}$	18	1.02	299.135	328.17	18	1.02	353.347	366.41
0^{LTS}	15	1.01325	1000.0	0.00[a]	15	1.01325	1000.0	0.00[a]
1^{LTS}	15.00	1.052	1000.0	0.057[a]	15.00	1.05	1000.0	0.054[a]
2^{LTS}	15.87	1.020	1000.0	0.093[a]	16.10	1.02	1000.0	0.132[a]
1^{CCU}	18	1.02	0.45748	2.88	18	1.02	0.37953	2.27
2^{CCU}	319.96	25	0.45748	4.72	320.0	25	0.37953	3.71
3^{CCU}	95	24.98	0.45748	4.09	95	24.98	0.37953	3.21
4^{CCU}	209.38	78.025	0.45748	4.70	209.4	78.025	0.37953	3.69
5^{CCU}	65	78	0.45427	4.33	65	78	0.37686	3.40
6	18	1.02	298.678	325.28	18	1.02	352.968	364.15
7	18	1.02	297.347	323.83	18	1.02	351.528	362.66
0^{Prod}	65	78	0.00321	0.0046	65	78	0.00266	0.0036
1^{Prod}	18	1.02	0.05381	0.059	18	1.02	0.30493	0.31
2^{Prod}	20.73	1.02	0.05702	0.062	18.42	1.02	0.30759	0.32
$0^{2\text{-}H2O'}$	18.99	30.9	1.03091	1.17	19.49	45.90	1.19000	1.30
$0^{2\text{-}H2O''}$	18.99	30.9	0.300	0.34	19.49	45.90	0.250	0.27
2^{H2O}	91.2	29.97	0.300	0.50	91.4	44.97	0.250	0.40

[a]Chemical exergy is not included in the LTS streams (HE2 cooling water).

Table 4

Main data for the power plant; Base Case, syngas and methane.

Fuel	syngas	methane
Fuel energy (LHV) rate (kW)	6627.2	6860.8
Fuel exergy rate (kW)	6757.8	7133.8
Flue gas exergy rate bleed to reactor (kW)	397.9	0
O_2 penalty, electric power (kW)	379.7	432.7
Delivered electric power (kW)	2117.4	2416.5
Captured/compressed CO_2, exergy rate (kW)	285.6	236.9
Exergy destruction rate (kW)	3700.4	4170.0
Overall exergy efficiency (%)	39.3	38.7

Table 5

Results for individual units of the process: Utilized exergy, exergy destruction (both in % of fuel chemical exergy) and exergy efficiency (%). Base Case, syngas and methane.

Unit	Fuel: syngas			Fuel: methane		
	$\frac{\Delta\dot{E}_{util}}{\dot{E}_{fu}^{ch}}$	$\frac{\dot{E}_d}{\dot{E}_{fu}^{ch}}$	ψ	$\frac{\Delta\dot{E}_{util}}{\dot{E}_{fu}^{ch}}$	$\frac{\dot{E}_d}{\dot{E}_{fu}^{ch}}$	ψ
HE1	5.80	2.46	57.5	6.42	2.67	58.5
HE2	0.85	0.82	4.2	1.02	0.94	7.7
HE3	0.63	0.16	73.9	0.49	0.13	73.9
HE4	0.37	0.21	42.7	0.29	0.17	43.1
WCC	109.96	43.31	60.6	109.00	45.64	58.1
C-Fuel	2.61	0.19	92.7	1.00	0.08	92.3
GT1	30.37	1.13	96.3	29.07	1.09	96.3
GT2	19.25	1.12	94.2	21.89	1.29	94.1
P	0.14	0.08	43.7	0.21	0.12	43.7
C1-CO2	1.96	0.13	93.5	1.54	0.10	93.5
C2-CO2	0.67	0.05	92.1	0.52	0.04	92.1
SEC	331.32	2.30	99.3	370.79	3.35	99.1
P-EC	2.74	0.54	80.2	3.06	0.61	80.2
P-LTS	0.13	0.08	43.0	0.13	0.07	43.0
mech. loss		0.56	99.0		0.55	99.0
generator		0.64	98.65		0.67	98.65
motors		0.98	85.0		0.94	85.0
overall		54.76	39.3		58.45	38.7

5.3. Varying temperature of combustor outlet (turbine inlet)

The first series of variation was of the WCC effluent temperature, i.e., turbine inlet temperature of GT1, ranging from 850 °C to 1150 °C. The distribution of exergy (in % of fuel chemical exergy) is shown in Fig. 2. The pressures were kept constant (as the Base Case), and so also the temperature of Stream 5 from HE1 and the mass flow rates of fuel and oxygen to the combustor and of the bleed to the reactor. Accordingly, the fuel compression, the O_2 penalty and the captured CO_2 were also constant. The mass flow rates of the HE2 cooling water and of Stream 3^{H2O} were kept constant, while the injection was varied with Stream 1^{H2O}.

The most prominent change with increased WCC temperature was the exergy destruction of the WCC, which decreased from 49.5% to 42.2% of the fuel chemical exergy. A higher temperature led to increased exergy in the bleed flow, from 4.6 to 6.2%. Higher turbine-inlet temperature led to higher power, in spite of a lower mass flow rate (less injected water). The exergy destruction of the gas turbines was slightly reduced, while that of HE1 increased a little (the effects of increased

temperature exceeded the effects of reduced flows). The sum of gas turbines and HE1 had a small increase (from 2.2 to 2.6%). The lower mass flow rate also led to slightly lower exergy destruction in the spray ejector condenser. The small sum of discharges was reduced from 0.27 to 0.25%. The net delivered electric power increased from 1.74 MW (25.8%) to 2.18 MW (32.3%).

A case similar to the Base Case (1100 °C) was also run, however without bleed to the gasifier. Then, the streams through GT2, HE1, SEC and CO_2 capture increased correspondingly. This case is also included
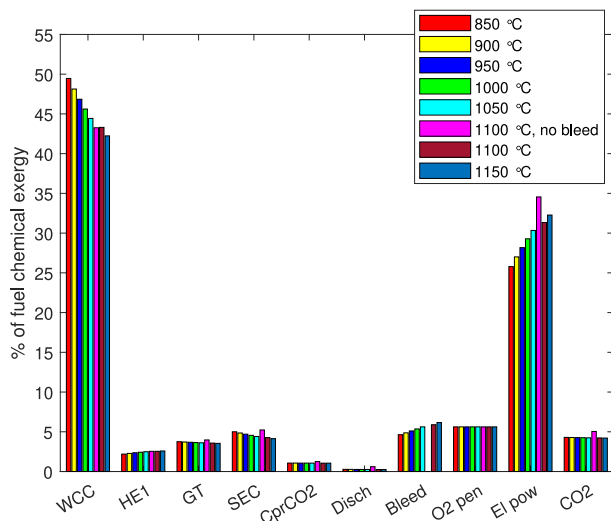
Fig. 2. Exergy distribution at varied turbine inlet temperature, syngas, including one case run without bleed. For the bar group labels, see Section 5.2.
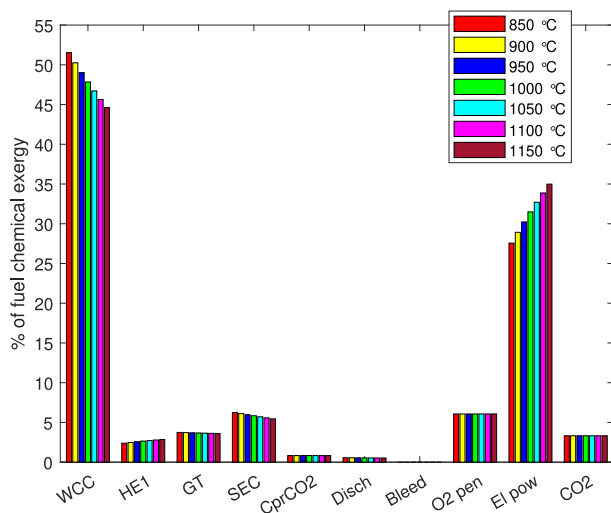

Fig. 3. Exergy distribution at varied turbine inlet temperature, methane, cf. Section 5.2.

Fig. 4. Exergy distribution at varied combustor pressure, syngas, cf. Section 5.2. The combustor-outlet temperature is also shown in the legend (cf. text of Section 5.4).

Fig. 5. Exergy distribution at varied combustor pressure, methane, cf. Section 5.2.

in Fig. 2. From the avoided bleed of 5.61% of fuel chemical exergy, the electric power delivery increased by 3.22%, and the additionally captured CO_2 represented 0.81%.

The corresponding results for methane are shown in Fig. 3.

5.4. Varying pressure of combustor

The fuel inflow was kept constant, and also the O_2 penalty (neglecting the small additional pumping power of liquid O_2 in the air-separation unit). For syngas, the variation was made for two levels of combustor temperature. This was because increasing combustor pressure also required an increase in injection-water pressure, which affected heat exchange and the energy balance of WCC. Since the WCC temperature here was a result rather than a parameter, maintaining a constant value over the entire range of pressure was complex.

The obvious and expected effects of increased pressure was the increased power of GT1. Since the pressure of Stream 3 (due to bleed) was kept constant, its temperature fell with increased WCC pressure (constant WCC outlet temperature). Thus, the bleed exergy was reduced. The overall exergy destruction had a small reduction with increasing pressure. The localization of exergy destruction shifted from combustor
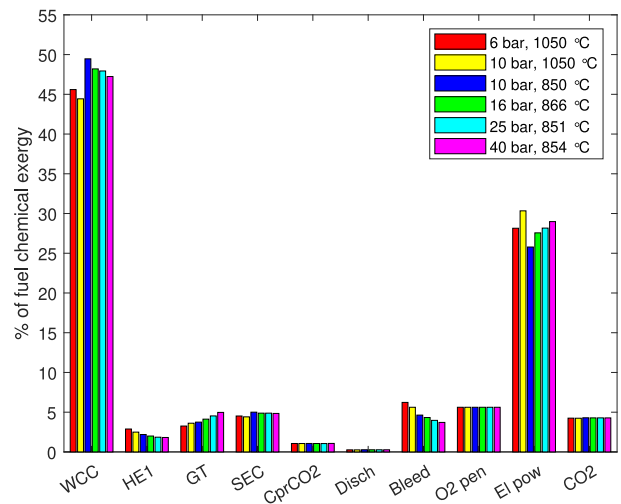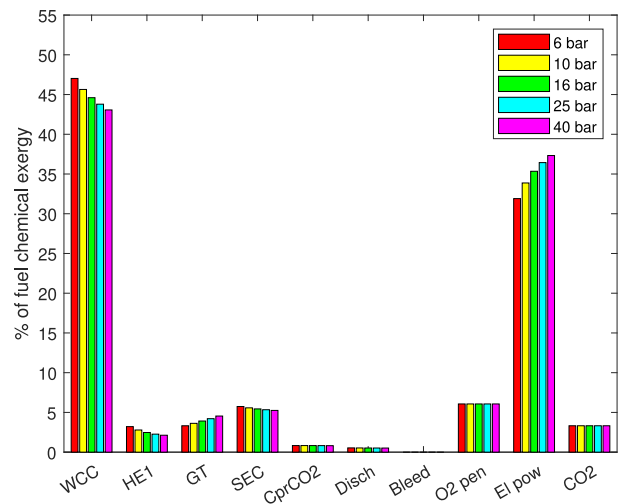
and HE1 to gas turbines and fuel compressors. Since pressure and temperatures of SEC inlets were constant, the exergy destruction there and in CO_2 separation and compression were unaltered.

The net effect of pressure increase was an increase in delivered power, as seen in Fig. 4. The results for methane are shown in Fig. 5.

5.5. Varying pressure and temperature of flue gas to spray ejector condenser

The GT2 exit pressure was varied from 0.068 (BC) to 0.10 bar (SEC inlet pressure 0.025 bar below these values), Fig. 6. Here the fuel, O_2, bleed and captured CO_2 amounts remained constant, and also temperature and pressure of the GT1 inlet and outlet and the GT2 inlet. The injected water flow rate and temperatures, and hence the flue gas flow rate, had very small changes. The main variation was the power and exergy outflow rate of GT2, due to the reduced expansion ratio. The lesser GT2 power directly influences the net delivered electric power. This led to a higher exergy flow rate to SEC (Stream 5). Since the condenser is mainly dissipating the thermomechanical exergy of Stream 5, its exergy destruction rate increased correspondingly.

Varying the temperature of flue gas flow to SEC (Stream 5) from 32 to 120 °C (BC: 40 °C) implies less heat transfer to WCC injection water in HE1. The fuel, O_2, bleed and captured CO_2 amounts remained
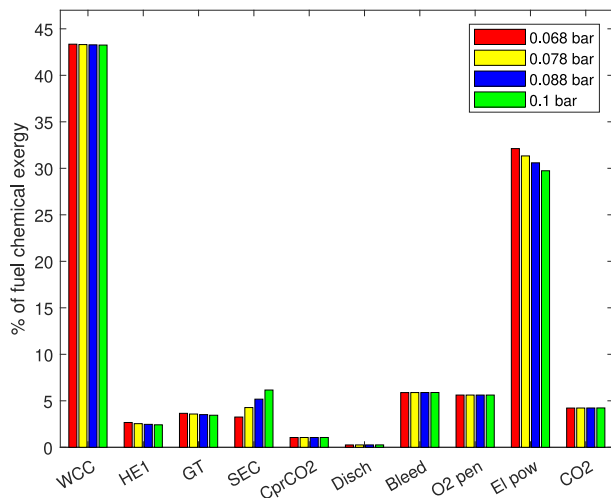
Fig. 6. Exergy distribution at varied GT2 exit pressure, syngas, cf. Section 5.2.
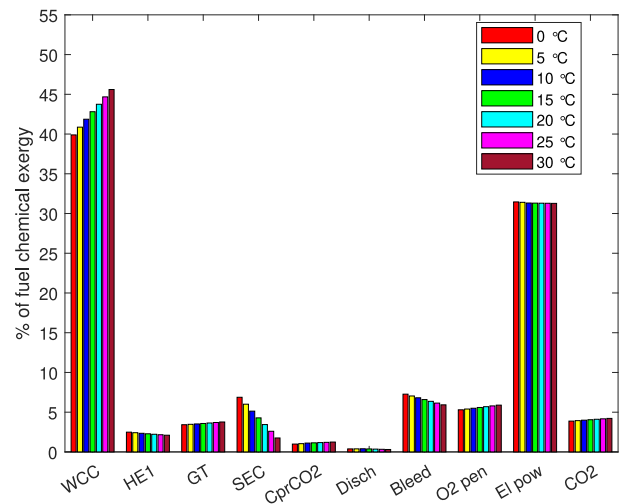

Fig. 8. Exergy distribution at varied ambient temperature, syngas, cf. Section 5.2.
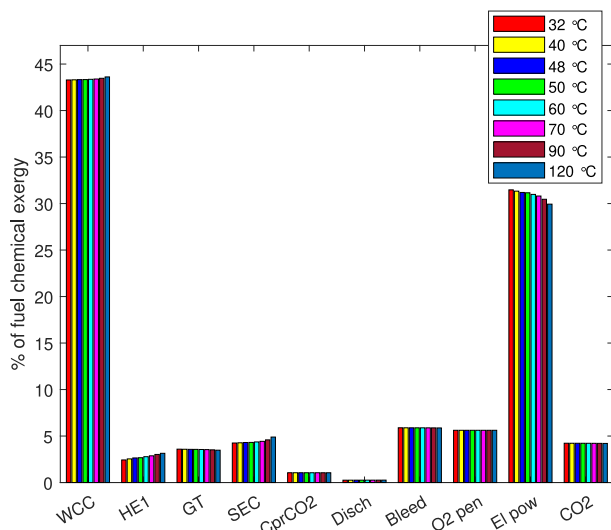

Fig. 7. Exergy distribution at varied flue gas temperature to SEC, syngas, cf. Section 5.2.
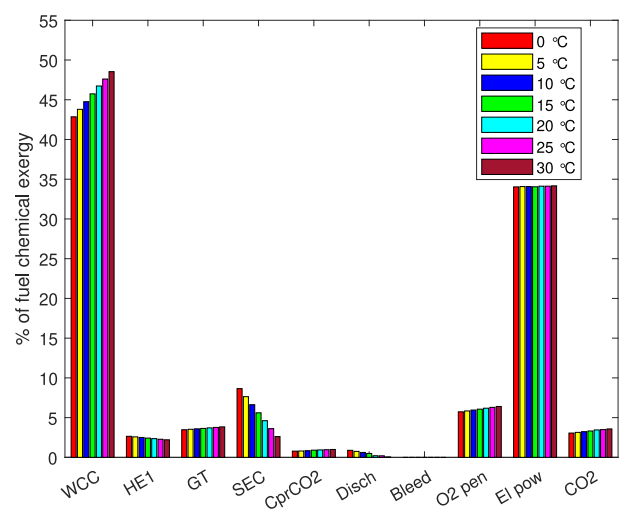

Fig. 9. Exergy distribution at varied ambient temperature, methane, cf. Section 5.2.

constant, and also temperature and pressure of GT1 inlet and outlet and the GT2 inlet. However, with lesser thermal energy of the water, a lesser mass flow rate is needed to obtain the constant WCC outlet temperature. This implies a lower flue gas mass flow rate and reduced power production in the gas turbines. Even though less heat is transferred in HE1, the exergy destruction rate increased, as the temperature differences increased (exergy efficiency fell from 60 to 45%). The flow exergy in flue gas to the condenser increased with its temperature, and hence the exergy destruction there. Exergy distribution results are shown in Fig. 7.

5.6. Varying pressure and temperature of condenser outlet

The variations of discharge pressure and temperature from SEC led to changes that were hardly distinguishable in the bar graphs and, therefore, not shown.

The pressure of the SEC outlet (Stream $2^{1\text{-SEC}}$) was varied from 1.0 to 1.105 bar (BC: 1.02 bar). The electric power delivery had a tiny increase of 0.11% of the fuel chemical exergy, which corresponded to the same reduction in exergy destruction. The spray ejector and its pump and motor contributed 0.10 of this percentage.

The condenser outlet temperature, Stream $2^{2\text{-SEC}}$, is also the temperature of Streams 6, 7, 0^{SEC}, 1^{CCU} and $0^{1\text{-H2O}}$, and it directly affects the temperatures of the SEC motive water and outlet, Streams 1^{SEC} and $2^{1\text{-SEC}}$, and of the WCC injection water before heating. The increase from 16 to 20 °C (BC: 18 °C) led to a tiny increase of electric power delivery by 0.10% of the fuel chemical exergy. The corresponding reduction of exergy destruction summarized from numerous small contributions, like HE1 (−0.09%), WCC (−0.04%), SEC group (+0.02%, including −0.69% for SEC and +0.71% for HE2), etc.

For both parameter variations, the combustor and units producing or consuming power were scarcely changed. Thus the main change was a redistribution of the dissipation in the condenser.

5.7. Ambient temperature variation

This was a variation in temperature of cooling water, fuel and O_2 supply. At the lowest temperature, 0.01 °C ("0 °C" for short), water was assumed not to freeze. Furthermore, the chemical exergies of the involved species were changed with T_0 [19]. The distribution of exergy (in % of fuel chemical exergy) is shown in Fig. 8 for syngas and in Fig. 9 for methane.

During the variation of T_0, the fuel and oxygen flow rates were kept constant. Also the state of the flue gas (Streams 2 to 5), and the bleed

mass flow rate, were constant. However, changes in thermal energy of injected water (temperature and flow rate) caused a small reduction in the flue gas mass flow rate with lower temperature, and hence of the produced turbine work: 1.4% reduction for Stream 2 from 30 to 0 °C and 1.8% for work. Over the same variation, chemical exergy of syngas was reduced by 0.9%, while that of the flue gas and bleed increased by 25%. The pressure and flow rate of captured CO_2 was constant.

The exergy efficiency of the oxygen supply (cf. Section 4.1) was kept constant at varying ambient temperature. Consequently, the O_2-penalty was scaled with T_0 compared to the Base Case.

For the combustor (WCC) at lower T_0, the outflow exergy of flue gas increased more than the increased inflow exergy of water, hence reduced exergy destruction.

For conventional thermal power processes, the power will usually increase with lower ambient temperature. The condenser pressure will decrease with lower coolant temperature. Furthermore, a conventional gas turbine will have an air compressor, which benefits from colder atmospheric air.

The present process does, of course, not have an air compressor. However, if the oxygen is produced in a cryogenic process, this process will benefit from lower temperature. Furthermore, the flue gas inlet pressure to the spray-ejector condenser depends on the momentum rate (i.e., pressure and mass flow rate) of the injected water, rather than the temperature of the cooling medium. Therefore, it shows no direct benefit from lower ambient temperature. Since the flow exergy of the flue gas increases with lower ambient temperature, the exergy destruction of the SEC increases.

In total, the net power delivery showed a small increase with lower ambient temperature (0.5% of fuel chemical exergy from 15 to 0 °C) for syngas, while an even smaller decrease for methane.

5.8. Oxygen penalty and bleed to gasification reactor

In this study, the source of oxygen was regarded as an air-separation unit outside the analysis, and an exergy penalty was assumed. Details of oxygen production was out of scope for the study here. The required power directly reduces the net electric power delivery from the plant.

The assumption relied on availability of technology, and the chosen value can be subject of discussion. An interesting future perspective is the expected implementation of hydrogen in the energy system. A possible source of oxygen can be the by-product from extensive hydrogen generation by electrolyzers. Potentially, industry will produce more pure O_2 than needed, and the marginal cost both in money and exergy might be low.

The gasifier was also regarded out of scope of this study. It was considered by the syngas fuel supply and the bleed of flue gas to the reactor. Since the bleed pressure was kept constant, variations of the GT1 effluent temperature lead to variation in bleed temperature and hence, its flow exergy. The fixed bleed pressure, i.e., fixed GT1 outlet pressure, limits the possibilities for optimal choices of expansion ratios. Furthermore, water injection variation also led to some chemical exergy variation of the flue gas. Potentially, increased bleed exergy could lead to improvement of the gasification reactor efficiency. This will, however, not be visible in the present analysis. Potentially, a higher bleed gas temperature could be utilized by heat exchange with WCC injection water. It would require another heat exchanger, with a pressure loss that would imply a reduced GT1 pressure ratio.

5.9. Overall discussion

Two important issues for the power plant are efficiency and size. First, fuel gasification and oxygen production are penalties that have to be satisfied. Moreover, capture and compression of CO_2 have a cost. Second, in this project, compactness is an aim. Comparing cycles of different studies can be difficult, as a wide range of choices and assumptions influence the performance. Even in comparisons on a common basis made by the same investigators using the same tools (e.g., [15]), similar assumptions can have different impact on different cycles. An important feature of the water cycle is its simplicity. Other cycles can have several compressors, heat exchangers and reactors (see e.g., [10,15]).

For instance, Habib et al. [33] pointed out that the water cycle is similar to the bottoming part of the Graz cycle (oxy-combustion with steam), and that the difference is that heat is added at much lower temperature. Therefore, lower efficiencies are reported. They did not mention the extensive compression of vapour in the Graz cycle.

A striking observation from the present analysis was the large fraction of exergy destruction pertaining to the combustor, nearly 80%. In comparison, the pre-combustion CO_2 capture power plant with natural gas reforming analyzed by [10] and the S-Graz cycle [34] had less than 70% in reactors. These cycles have a multitude of other units.

In the wet combustion chamber, the injected water can be assumed to evaporate at the saturation temperature of the combustor pressure. That is, at 180 °C for 10 bar or 250 °C at 40 bar. A relevant question is whether evaporation by low-grade heat before injection would be better. Obviously, utilizing combustion heat at these temperatures implies notable exergy destruction. Approximately half the reaction heat release was captured by evaporation, while the other half was captured by temperature increase. Consequently, external evaporation would require, roughly, twice the amount of water. The necessary amounts of low-grade heat are, simply, not available in the system. Using higher-temperature heat would counteract the idea behind the external evaporation. Moreover, evaporation outside the combustor would still require notable temperature differences for the heat transfer, with the associated exergy destruction. As a side effect, a relatively large heat exchanger (boiler) would be required.

Results of some parameter variations can be seen as expected and even felt as intuitive. Several authors have formulated guidelines to explain and guide design of thermo-chemical systems based on the 2nd law, for instance the "12 commandments" by Leites et al. [35] and 20 "practical rules" by Szargut [36], both accompanied by background and reasoning. The large exergy destruction in the combustor is explained by several "commandments" (e.g., No. 1 about driving forces, No. 3 about exothermic reactions and No. 6 about mixing of different flows [35]) and "rules". Simplicity of the process is acknowledged by "Rule 16" [36], on not to elongate the chain of processes.

Increasing the combustor outlet/turbine inlet temperature gave the most predictable result: slightly more turbine work output and reduced exergy destruction in the combustor. On the other hand, the increased combustor pressure did not fully align with the guidelines: reactions with decreasing volume should, according to "Commandment 4" [35], give less exergy destruction at lower pressure, not vice versa as indicated in Fig. 4. In the present case, the increased water evaporation temperature may have had a greater and opposite effect.

Even though the thermodynamics clearly suggests that increasing temperature and pressure are beneficial, the practical conditions of material properties etc. may challenge those options.

6. Concluding remarks

A power cycle with water oxy-combustion of syngas or methane and CO_2 capture is investigated by exergy analysis. The size of the power plant was about 2 MW electric power. The plant is intentionally kept compact, with no reheat and using a spray ejector condenser (SEC).

* The net delivered electric power was 31% of the syngas fuel exergy. When flue gas bleed to the gasifier and O_2 separation penalty are considered, the exergy task efficiency is 39%, including the exergy of captured CO_2 in the useful product. The combustor is the dominating source of irreversibility, with 80% of the exergy destruction. Increasing the combustor outlet (turbine inlet) temperature reduced the combustor and overall exergy destruction and increased efficiency. The same effects were seen when increasing the combustor pressure.

* Increasing the pressure of the flue gas exiting the last gas turbine (inlet to SEC) increased SEC exergy destruction and reduced the turbine power and cycle efficiency, without affecting much the other units. Increasing the temperature of the same stream had similar effects.

* Variation of the SEC outlet temperature and pressure had small effects other than redistributing exergy destruction among units related to SEC.

* Reducing the ambient temperature, essentially the condenser cooling water temperature, leads to a nearly unchanged overall efficiency, contrary to conventional steam cycles and gas-turbine combined cycles. The reason is that the pressure of the flue gas inlet to the SEC depends on the pressure and mass flow of the injected liquid rather than the cooling water temperature.

CRediT authorship contribution statement

Ivar S. Ertesvåg: Conceptualization, Methodology, Validation, Formal analysis, Investigation, Writing – original draft, Writing – review & editing, Visualization. **Paweł Madejski:** Conceptualization, Methodology, Validation, Formal analysis, Investigation, Writing – review & editing. **Paweł Ziółkowski:** Conceptualization, Writing – review & editing. **Dariusz Mikielewicz:** Conceptualization, Writing – review & editing.

Declaration of competing interest

The authors declare that they have no known competing financial interests or personal relationships that could have appeared to influence the work reported in this paper.

Data availability

Data will be made available on request.

Acknowledgments

References

[1] Negative CO2 emission gas power plant. 2019, URL https://nco2pp.mech.pg.gda.pl/eng, (Accessed 15 2022).

[2] Ziółkowski P, Madejski P, Amiri M, Kuś T, Stasiak K, Navaneethan NS, et al. Thermodynamic analysis of negative CO2 emission power plant using Aspen Plus, Aspen Hysys, and Ebsilon software. Energies 2021;14. http://dx.doi.org/10.3390/en14196304.

[3] Ganjehkaviri A, Mohd Jaafar M, Ahmadi P, Barzegaravval H. Modelling and optimization of combined cycle power plant based on exergoeconomic and environmental analyses. Appl Therm Eng 2014;67:566–78. http://dx.doi.org/10.1016/j.applthermaleng.2014.03.018.

[4] Mokhtari H, Ahmadisedigh H, Ameri M. The optimal design and 4E analysis of double pressure HRSG utilizing steam injection for Damavand power plant. Energy 2017;118:399–413. http://dx.doi.org/10.1016/j.energy.2016.12.064.

[5] Ziółkowski P, Kowalczyk T, Lemański M, Badur J. On energy, exergy, and environmental aspects of a combined gas-steam cycle for heat and power generation undergoing a process of retrofitting by steam injection. Energy Convers Manage 2019;192:374–84. http://dx.doi.org/10.1016/j.enconman.2019.04.033.

[6] Cassetti G, Rocco M, Colombo E. Exergy based methods for economic and risk design optimization of energy systems: Application to a gas turbine. Energy 2014;74:269–79. http://dx.doi.org/10.1016/j.energy.2014.07.043.

[7] Soufi MG, Fujii T, Sugimoto K. A modern injected steam gas turbine cogeneration system based on exergy concept. Int J Energy Res 2004;28:1127–44. http://dx.doi.org/10.1002/er.1019.

[8] Amrollahi Z, Ertesvåg IS, Bolland O. Optimized process configurations of post-combustion CO2 capture for natural-gas-fired power plant – Exergy analysis. Int J Greenh Gas Contol 2011;5:1393–405. http://dx.doi.org/10.1016/j.ijggc.2011.09.004.

[9] Mondino G, Spjelkavik AI, Didriksen T, Krishnamurthy S, Stensrød RE, Grande CA, Nord LO, Blom R. Production of MOF adsorbent spheres and comparison of their performance with zeolite 13X in a moving-bed TSA process for postcombustion CO2 capture. Ind Eng Chem Res 2020;59:7198–211. http://dx.doi.org/10.1021/acs.iecr.9b06387.

[10] Ertesvåg IS, Kvamsdal HM, Bolland O. Exergy analysis of a gas-turbine combined-cycle power plant with precombustion CO2 capture. Energy 2005;30:5–39. http://dx.doi.org/10.1016/j.energy.2004.05.029.

[11] Mohammadpour M, Houshfar E, Ashjaee M, Mohammadpour A. Energy and exergy analysis of biogas fired regenerative gas turbine cycle with CO2 recirculation for oxy-fuel combustion power generation. Energy 2021;220:119687. http://dx.doi.org/10.1016/j.energy.2020.119687.

[12] Okeke IJ, Ghantous T, Adams TA. Design strategies for oxy-combustion power plant captured CO2 purification. Chem Prod Proc Model 2021. http://dx.doi.org/10.1515/cppm-2021-0041.

[13] Fu C, Gundersen T. Using exergy analysis to reduce power consumption in air separation units for oxy-combustion processes. Energy 2012;44:60–8. http://dx.doi.org/10.1016/j.energy.2012.01.065.

[14] Bolland O, Kvamsdal HM, Boden JC. A thermodynamic comparison of the oxy-fuel power cycles water-cycle, Graz-cycle and Matiant-cycle. In: Proc. Power generation and sustainable development, 8-9 2001, Liège, Belgium. 2001, p. 293–8.

[15] Kvamsdal HM, Jordal K, Bolland O. A quantitative comparison of gas turbine cycles with CO2 capture. Energy 2007;32:10–24. http://dx.doi.org/10.1016/j.energy.2006.02.006.

[16] Martinez-Frias J, Aceves SM, Smith JR, Brandt H. Thermodynamic analysis of zero-atmospheric emissions power plant. ASME J Eng Gas Turbines Power 2004;126:2–8. http://dx.doi.org/10.1115/1.1635399.

[17] Ust Y, Ozsari I. Exergetic performance analysis to compare of two different oxy fuel combustion power plant. In: Int. conf. engineering and natural sciences (ICENS), Prague, Czech Republic, 12-16 2019. 2019, p. 281–93.

[18] Steag energy services - Ebsilon professional 15.00. 2021, URL http://www.ebsilon.com, (Accessed 10 2022).

[19] Ertesvåg IS. Sensitivity of the chemical exergy for atmospheric gases and gaseous fuels to variation in ambient conditions. Energy Convers Manage 2007;48:1983–95. http://dx.doi.org/10.1016/j.enconman.2007.01.005.

[20] Szargut J, Morris DR, Steward FR. Exergy analysis of thermal, chemical, and metallurgical processes. 1988, Hemisphere, New York.

[21] International Organization for Standardization. Gas turbines – Acceptance tests. Technical Report ISO 2314:2009(E), 3rd ed.. ISO; 2009.

[22] Ziółkowski P, Badur J, Pawlak-Kruczek H, Stasiak K, Amiri M, Niedzwiecki L, Krochmalny K, Mularski J, Madejski P, Mikielewicz D. Mathematical modelling of gasification process of sewage sludge in reactor of negative CO2 emission power plant. Energy 2022;244:122601. http://dx.doi.org/10.1016/j.energy.2021.122601.

[23] Ziółkowski P, Stasiak K, Amiri M, Mikielewicz D. Negative carbon dioxide gas power plant integrated with gasification of sewage sludge. Energy 2023;262:125496. http://dx.doi.org/10.1016/j.energy.2022.125496.

[24] Sammak M, Thern M, Genrup M. Performance of a semi-closed oxy-fuel combustion combined cycle (SCOC-CC) with an air separation unit (ASU). In: Volume 3: Coal, biomass, and alternative fuels; cycle innovations; electric power; industrial and cogeneration; organic rankine cycle power systems, turbo expo: power for land, sea, and air; Oslo, Norway, 11-15 Jun. 2018. 2018, p. 1–10. http://dx.doi.org/10.1115/GT2018-76218, v003T06A010.

[25] Singla R, Chowdhury K. Comparisons of thermodynamic and economic performances of cryogenic air separation plants designed for external and internal compression of oxygen. Appl Therm Eng 2019;160:114025. http://dx.doi.org/10.1016/j.applthermaleng.2019.114025.

[26] Soave G. Equilibrium constants from a modified Redlich-Kwong equation of state. Chem Eng Sci 1972;27:1197–203. http://dx.doi.org/10.1016/0009-2509(72)80096-4.

[27] Ibrahim M, Skaugen G, Ertesvåg IS, Haug-Warberg T. Modeling CO2-water mixture thermodynamics using various equations of state (EoSs) with emphasis on the potential of the SPUNG EoS. Chem Eng Sci 2014;113:22–34. http://dx.doi.org/10.1016/j.ces.2014.03.025.

[28] International association for the properties of water and steam, IAPWS R7-97. 2012, URL http://www.iapws.org/relguide/IF97-Rev.html, (Accessed 5 2022).

[29] Nami H, Ertesvåg IS, Agromayor R, Riboldi L, Nord LO. Gas turbine exhaust gas heat recovery by organic rankine cycles (orc) for offshore combined heat and power applications - energy and exergy analysis. Energy 2018;165:1060–71. http://dx.doi.org/10.1016/j.energy.2018.10.034.

[30] Rian AB, Ertesvåg IS. Exergy evaluation of the arctic snøhvit liquefied natural gas processing plant in northern Norway–significance of ambient temperature. Energy Fuels 2012;26:1259–67. http://dx.doi.org/10.1021/ef201734r.

[31] Brodyanski VM, Sorin MV, Le Goff P. The efficiency of industrial processes: exergy analysis and optimization. Elsevier; 1994.

[32] Magnanelli E, Berglihn OT, Kjelstrup S. Exergy-based performance indicators for industrial practice. Int J Energy Res 2018;42:3989–4007. http://dx.doi.org/10.1002/er.4123.

[33] Habib MA, Badr HM, Ahmed SF, Ben-Mansour R, Mezghani K, Imashuku S, la O' GJ, Shao-Horn Y, Mancini ND, Mitsos A, Kirchen P, Ghoneim AF. A review of recent developments in carbon capture utilizing oxy-fuel combustion in conventional and ion transport membrane systems. Int J Energy Res 2011;35:741–64. http://dx.doi.org/10.1002/er.1798.

[34] Nami H, Ranjbar F, Yari M. Thermodynamic assessment of zero-emission power hydrogen and methanol production using captured CO2 from S-Graz Oxy-Fuel cycle and renewable hydrogen. Energy Convers Manage 2018;161:53–65. http://dx.doi.org/10.1016/j.enconman.2018.01.054.

[35] Leites I, Sama D, Lior N. The theory and practice of energy saving in the chemical industry: some methods for reducing thermodynamic irreversibility in chemical technology processes. Energy 2003;28:55–97. http://dx.doi.org/10.1016/S0360-5442(02)00107-X.

[36] Szargut J. Exergy method: technical and ecological applications. Southhampton UK: WIT Press; 2005.